



Progress towards the validation of SIMMER-III code model for lead-lithium water chemical interaction

Satya Prakash Saraswat^{a,*}, Vittorio Cossu^a, Francesco Galleni^a, Marica Eboli^b,
Alessandro Del Nevo^b, Nicola Forgiione^a

^a DIC1 – University of Pisa, Largo Lucio Lazzarino 2, Pisa 56122, Italy

^b ENEA FSN-ING-SIS, CR Brasimone, Camugnano, BO 40032, Italy

ARTICLE INFO

Keywords:

WCLL
SIMMER-III
Lead-lithium
LIFUS5/Mod3 facility
Code validation
Multi-phase flow
Chemical interaction

1. Introduction

The Water-Cooled Lithium Lead (WCLL) BB is being investigated as a potential option for the foremost breeding blanket technology in the construction of the European DEMO nuclear fusion reactor [1–3] and has recently been considered in the ITER Test Blanket Module (TBM) program [4]. The interaction between PbLi and water induced by a tube rupture in the breeding zone, known as an in-box LOCA (Loss of Coolant Accident), is a crucial safety problem for the design of this component [4–8]. This phenomenon was studied to generate comprehensive, reliable data for validating system code used in deterministic safety studies [4–8]. Indeed, a qualified code is critical for evaluating the unintentional effects, selecting potential mitigating actions, and offering design alternatives to minimize harm to the blanket box structures [9,10].

Due to a combination of thermal and chemical interactions, water discharge into liquid metals results in a significant energy release that further contributes to pressure and temperature increases. How this chemical reaction owing to water leakage into the lead-lithium could breach the blanket box, or whether this possibility can be ruled out, is a

concern that affects the WCLL blanket conceptual design. Research is continued to better understand the phenomena and mechanisms involved during the supposed in-box LOCA to overcome the WCLL BB system's safety response, improve the predictive capabilities of numerical tools, and validate computer models, codes, and techniques for their applicability. Furthermore, the dependability of certified system code for deterministic safety analysis is critical considering the evaluation of unintentional effects and dampening interventions. To complement these actions, the current state of knowledge necessitates observational data.

Nonetheless, separate effect tests have been performed in the past, but they were not meant to do DSA code validation and verification. As a result, the Series E experimental campaign has begun, and the new distinct effect test facility LIFUS5/Mod3 [4,6–8] has been commissioned.

The Series-E experimental campaign has been developed to accurately recreate the LOCA scenario, from the rupture in the water channel up to the complete equilibrium between the water line and the BB box, to better understand these phenomena related to the safety of the

Abbreviations: BB, breeding blanket; DEMO, DEMOnstration fusion reactor; DP, differential pressure transducer; ENEA, Italian national agency for new technologies, energy and sustainable economic development; EOI, end of injection; EOT, end of transient; LV, level; MT, mass flow meter; P&ID, plan and instrumentation diagram; PbLi, lead-lithium alloy; PC, pressure transducer absolute GE DRUCK type; PT, pressure transducer fast and dynamic Kistler type; S1B, reaction vessel; SBL, injection system; SET, separate effect test; SG, strain gage; SOT, start of transient; TC, thermocouple, acquisition and control type; VA, automatic valve; VE, electrovalve; VM, manual valve; VP, pneumatic valve; VS, safety valve; WCLL, water cooled lead lithium.

* Corresponding author.

E-mail address: satya.saraswat@ing.unipi.it (S.P. Saraswat).

<https://doi.org/10.1016/j.fusengdes.2023.113819>

Received 3 October 2022; Received in revised form 7 May 2023; Accepted 12 May 2023

Available online 16 May 2023

0920-3796/© 2023 The Authors. Published by Elsevier B.V. This is an open access article under the CC BY license (<http://creativecommons.org/licenses/by/4.0/>).

WCLL BB design. The LIFUS5/Mod3 facility has been upgraded to do this. One of the critical tests in the Series-E experimental campaign is Test E5.2; the specifics of Test E will be covered in the next section.

The current paper thoroughly examines the Test E5.2 experimental data and its numerical post-test simulations with the SIMMER-III system code.

The main purpose of performing this post-test simulation of Test E 5.2 with SIMMER-III code and analysis of experiment is to confirm the code's ability to forecast the behavior of thermodynamic and chemical interactions of lead-lithium and water under conditions like those that could potentially occur in WCLL in-box LOCA. The findings are analyzed critically, showing the experimental framework's flaws, possibilities, numerical model's limitations, and capabilities.

The experiments aim to generate experimental data for validating SIMMER codes for fusion applications that have been changed. The Verification and Validation activities [11,12] necessitate the application of a standard technique to empirical observations and data with repeatable and specified baseline and operating conditions in order to achieve this goal. Simultaneously, a numerical simulation is being carried out using a modified version of the SIMMER-III algorithm, which implements the PbLi/water chemical interaction. The experimental results will also be used to promote the development of a new STH/2D coupled computation tool. Furthermore, the obtained information will be utilized to explore the dynamic impacts of energy release on structures and give useful input for further experimental campaigns. Aside from the design of the water and PbLi circuits, the BB box's various physical processes are solely dependent on the quantity of water injected into it. Some of these phenomena are listed below:

- The pressure differential between the PbLi and water circuits, which is the transient's primary factor; once the pressures in the two systems are balanced, the injection ceases.
- water flow behavior: the occurrence of blocked flow may restrict the flow rate of the water itself, while the phase of the stream will impact the total infused mass; the magnitude of the break, which results in a varied pressure loss that places a limit on the transient's velocity.

2. LIFUS5/Mod3 facility description

LIFUS5/Mod3 is an improvement over LIFUS5/Mod2 in its prior

form [11] to facilitate the new series D and E experimental campaigns. The present reaction vessel, the S1A, the water storage tank (SBL), and the expansion container (S3) are all still in use. According to the PED guideline, a relatively small reaction vessel (S1B) has been fitted and is appropriate for use at pressures and temperatures up to 200 bars and 500°C. The S3 dump vessel is shared between both parts of the facility and used in case of rupture disk activation to collect either cover gas or other substances released from the interaction vessels. The following description only concerns part B of the facility, which is committed in EUROfusion Consortium and uses S1B reaction vessel for PbLi/Water interaction experiments. The five main components of the facility are:

- The primary reaction vessel (S1B), in which the interaction involving liquid lead-lithium and water takes place.
- Vessels for injection and storing water: An injection line links the bottom of SBL to the bottom of S1B, and the SBL cylinder is used to store and bring water to experimental conditions.
- An argon cylinder attached to the top of the SBL maintains pressure throughout the period of injection.
- To protect the experimental setup in the event of overpressure, emergency expansion tank S3 is linked to S1B with 2 rupture plates.
- S4B1 and S4B2 lead-lithium storage vessels for pure and used alloy.
- Test section

Literature [5] describes the LIFUS5/Mod3-section B in detail. Fig. 1 shows the synoptic of LIFUS5/Mod3 experimental facility. The significant facility component parameter values are described in Table 1. The top flange, the lateral shell, and the lateral shell's strain gages are all mechanically equipped externally with thermocouples. All the S1B vessel's associated parts, Plan and Instrumentation Diagram (P&ID) and measurements sensors are listed in Table 1 and Fig. 2.

The test section, designed to have an axial-symmetric structure, is welded onto the top flange of S1B (see Fig. 3). A holed plate defines the area where lead-lithium and water interact. The subcooled water jet contacting the plate collapsed, forcing the water to interact with the PbLi. Also, the holes let the hydrogen and vapor made by the process rise to the top of the S1B vessel's upper plenum. However, the frame's flat side is entirely open. On the radial surface of the container, the strain gauges and adaptive pressure sensors are thus mounted to capture the pressure and the shock loads, respectively.

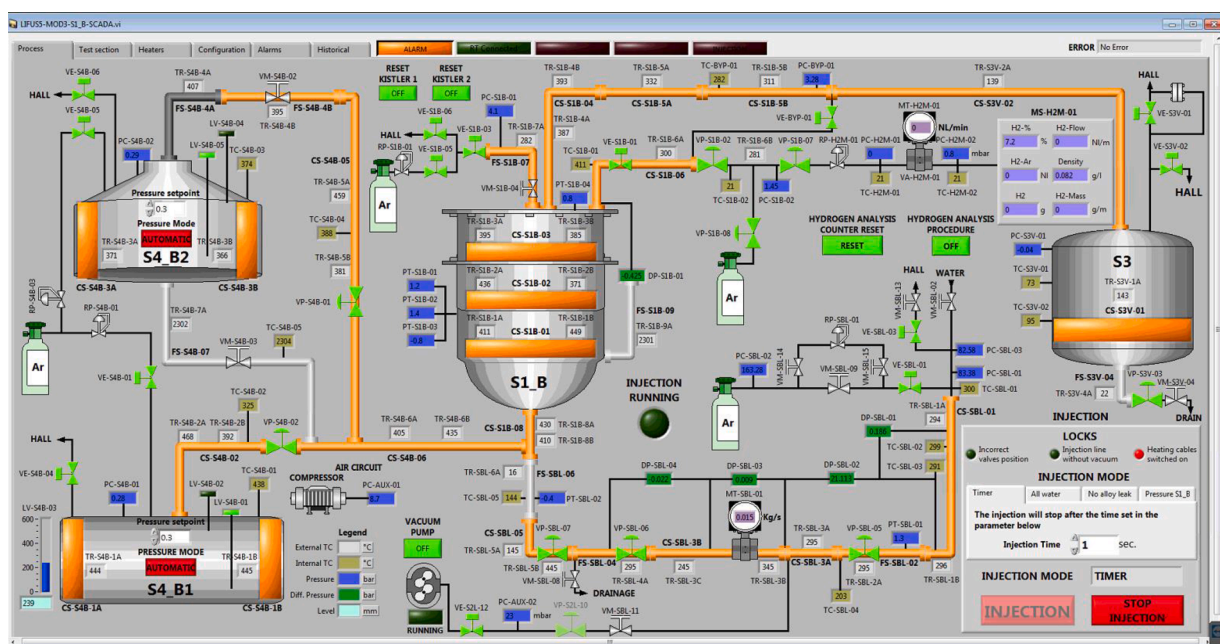


Fig. 1. LIFUS5/Mod3 facility, synoptic.

Table 1
significant facility component parameter values.

Component	Parameter	Value	
S1B Reaction vessel	Volume [m ³]	0.03	
	Inner diameter [m]	0.257	
	Height [m]	0.5555	
SBL Water pipe	Volume [m ³]	0.00263	
	Inner diameter [m]	0.03398 (lower section), 0.0094 (upper section)	
	Length [m]	2.8(lower section), 1.268(upper section)	
S3 Dump vessel	Volume [m ³]	2.0	
	Inner diameter [m]	1	
	Length [m]	2.8(lower section), 1.268(upper section)	
S4B2 Depleted PbLi storage tank	Volume [m ³]	0.40	
	Diameter [m]	0.544	
	Length [m]	1.56+hemispherical ends	
Injection line from SBL to S1B	Volume [m ³]	0.000395	
	Inner Diameter [m]	0.0094	
	Length [m]	5.69	
Expansion line from S1B to S3	Volume [m ³]	0.00858	
	Pipe Inner Diameter [m]	0.0429 (lower section), 0.0666 (upper section)	
	Length [m]	4.25 (lower section), 0.7 (upper section)	
Hydrogen line from S1B to H ₂ Analyser	Volume [m ³]	0.000157	
	Inner Diameter [m]	0.00434	
	Length [m]	10.62	
S4B1 Fresh PbLi storage tank	Volume [m ³]	0.40	
	Diameter [m]	0.544	
	Length [m]	1.56+hemispherical ends	
Instrumentation S1B	No.	Diameter	Utilization
Steel pipe	1	2"	Water injection and PbLi charging/ discharging system
Steel pipe	1	2"	Connection to S3-expansion/dump vessel
Test section TCs	1	1"	Gooseneck sealing system to TC passage
MS-H2M-01	1	½"	Hydrogen measurement system
DP-S1B-01	1	½"	DP meter and PC pressure transducer
PC-S1B-01	1	½"	PT KIESTLER pressure transducer
PT-S1B-04	3	½"	PT KIESTLER on cylindrical shell
DP-S1B-01	1	½"	DP meter
SG-S1B-02/03/04	3	–	Strain gages (circumferential), mounted on surface of vessel
SG-S1B-05	1	–	Strain gages (axial), mounted on surface of vessel
SG-S1B-01	1	–	Strain gages (radial), mounted on surface of vessel

As shown in Fig. 3, there are six levels between the injection system and the punched sheet where 0.5 mm thick thermocouples are placed. Fig. 4 shows real pictures of LIFUS5/Mod3 facility during the commissioning phase.

2.1. Test E5.2

The E5.2 Test was conducted using the experimental equipment

LIFUS5/Mod3 of CR Brasimone (ENEA) on May 13, 2021, and the results are presented in this manuscript. In fact, it can provide: (1) all available experimental data collected by the data acquisition device; (2) relevant data to the initial conditions and the test boundary; (3) a preliminary analysis and interpretation of the data, and (4) the data required for a more detailed analysis and execution of the post-test analysis using computational codes.

Water at 141.6 bars and 255.2 °C was injected in reaction vessel S1B containing lead-lithium eutectic. The experimental investigation examines the evolution of the pressure and temperature transients and the hydrogen produced by the chemical interaction between the two fluids. These results will be used to verify the chemical model of the lead-lithium-water reaction built in the SIMMER program. The important parameters and boundary conditions designed, during experimental execution and inputs to SIMMER-III are listed in Table 2.

3. SIMMER-III model

The numerical investigations were carried out using "SIMMER-III Ver. 3F Mod. 0.1" [13], a code version updated at the University of Pisa for fusion applications [14] by including the PbLi/Water chemical reaction model [15]. Post-test simulations are mostly used to validate and check the current chemical model in the code version. Examining the code model changes is needed in light of the post-analysis, experimental results, and comparison to more closely replicate the experimental results. After the experiment test E5.2 analysis, various numerical calculations are simulated for multiple values of orifice discharge coefficients and lead-lithium-water reaction rate coefficients (which are very dynamic due to their dependence on system thermal-hydraulic state, fluid flow regimes, and system geometry) [16]. The findings of this stage validate and verify the SIMMER code, especially for the particular conditions that have been used in experiment Test 5.2. Table 2 shows the test matrix data and other input conditions of experiment test E5.2, which have been used as initial and boundary conditions for the reference input of the LIFUS5/Mod3SIMMER-III thermal-hydraulic model.

In cylindrical coordinates, the thermal-hydraulic nodalization comprises 50 radial and 100 axial cells (see Fig. 5).

The following are the critical SIMMER-III code approaches and flags for numerical calculations:

- Inter-cell heat transmission occurs among all liquid components and solid particles, as well as between vapor, liquid components, and structures [17].
- To avoid numerical computations becoming unstable, the vapor temperature in two-phase cells with a tiny void percentage was adjusted.
- All relevant flags are configured to incorporate the turbulence-diffusion term and molecular momentum diffusion.
- The friction in the injector line was ignored in the chemical interaction model calculations since the SIMMER-III program estimates friction only in the mesh cells where the "can wall" constructions are incorporated.
- The injector device's orifice is where the concentrated pressure lowers owing to geometrical discontinuities. The exact location of injector orifice in SIMMER coordinates is (i=1to3 (radial) and j=45–47 (axial)).
- The input file's orifice coefficient of enlargement/constriction and curves are derived using empirical correlations as described in reference [18] to incorporate their best values, but they are susceptible to errors; therefore, a separate sensitivity analysis was also performed to find out their optimized values (not presented here). For the numerical analysis of the system to be done, the system's parts, such as the nodalization cells, need to be optimized. Along with the physical instability of the system, there are problems with the system code SIMMER-III due to: (a) the ill-posed nature of its two-fluid model in some of the transient two-phase flow fluid

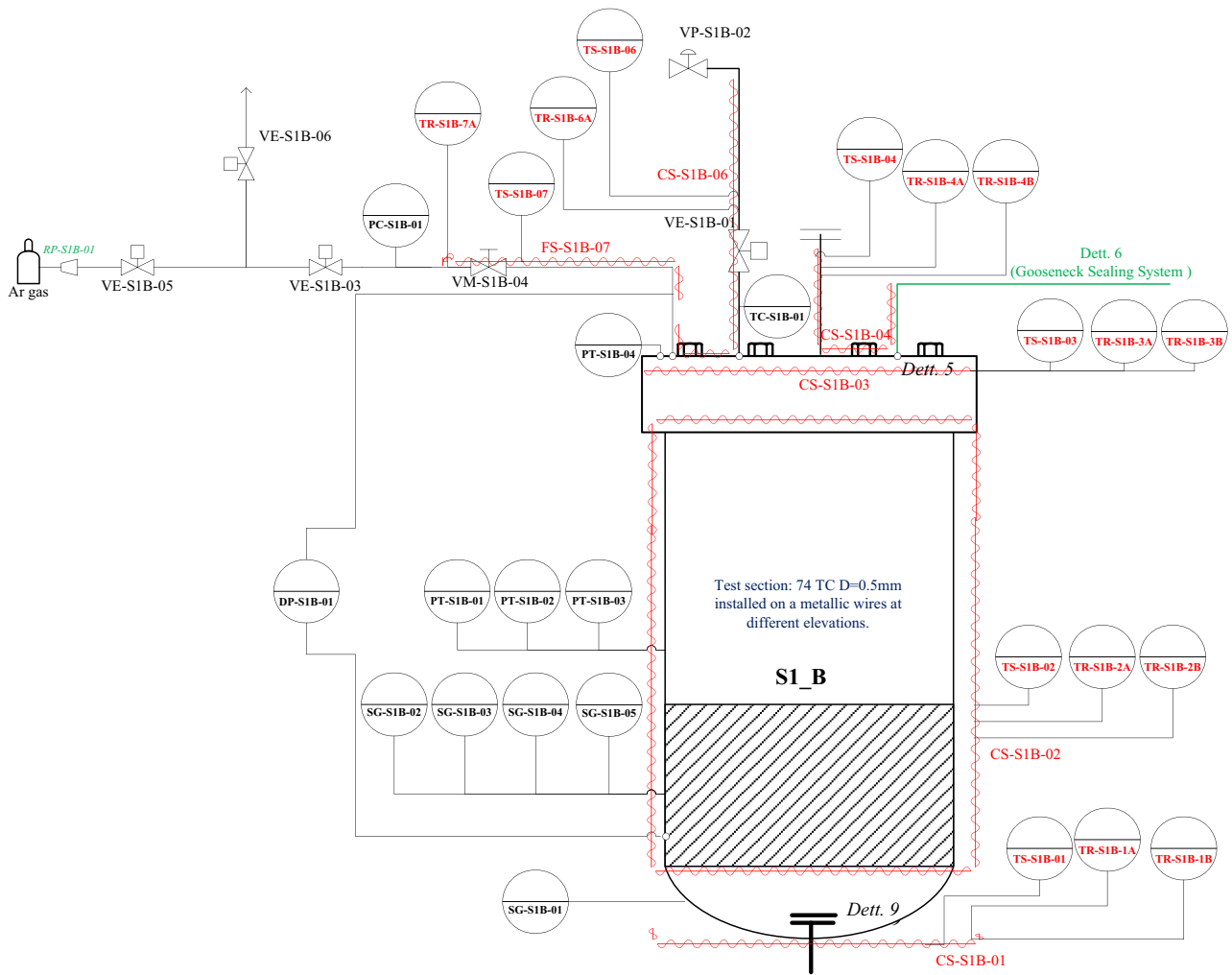


Fig. 2. LIFUS5/Mod3 facility, Plan and Instrumentation Diagram of S1B.

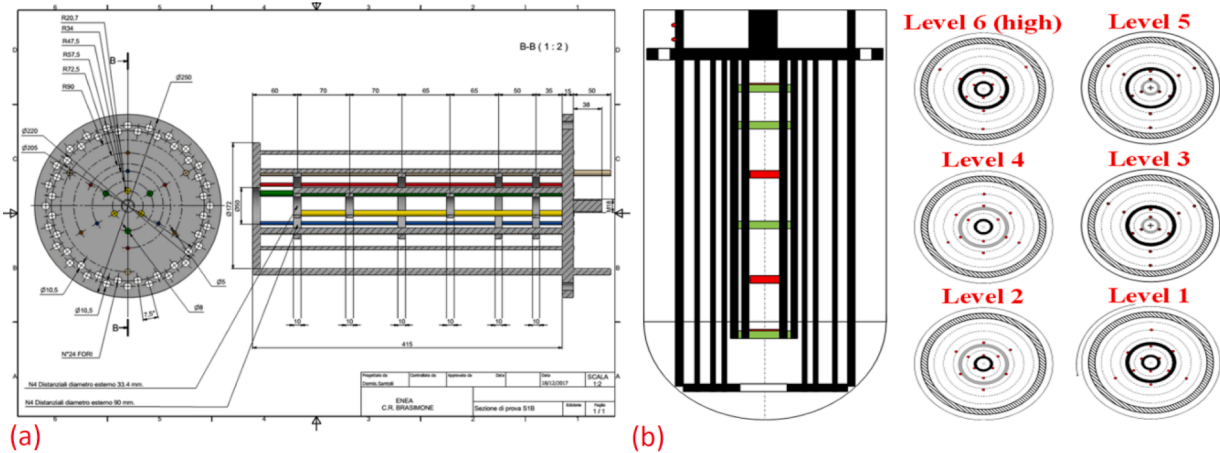


Fig. 3. LIFUS5/Mod3 facility Test section (a), sketch of Test section, (b) LIFUS5/Mod3 facility, layout of thermocouples in test section.

conditions, and (b) numerous different estimations like volume averaging, area averaging, and flow regime approximations (to optimize the required system memory and speed up the simulation process).

In this analysis, we choose the mesh size of a particular part so that the code can consider the physical instabilities and avoid the numerical instabilities that don't have to do with physics. The mesh size is chosen by analyzing the papers [19–21] and trying out different sizes.

In the literature [19–21], these non-physical numerical instabilities during simulations of two-phase flow have been discussed.



Fig. 4. Real pictures of LIFUS5/Mod3 facility during commissioning phase.

4. Results and discussion

The post-test analysis of LIFUS5/Mod3 Test 5.2 has been performed using SIMMER-III stand-alone system code. The reference input deck is developed based on the geometrical conditions given in Tables 1 and 2.

The boundary and the input conditions to the thermal-hydraulic model of the system are taken from Table 2 and time dependent input conditions are taken from the experimental data obtained (inlet pressure and temperature). The modeling conditions, correlations for various thermo-dynamic and heat flow phenomena, lead-lithium-water chemical interaction model and equation of states model considered for the analysis is considered from various literature [8–13]. The primary

results obtained using the numerical simulations of test E5.2 are summarized and discussed in this section. There are four distinct major phenomenological stages to the simulated and experimental transient. The linked dynamical trends and the subsequent sequence of events of the post-test and experimental results are presented in Figs. 6–9.

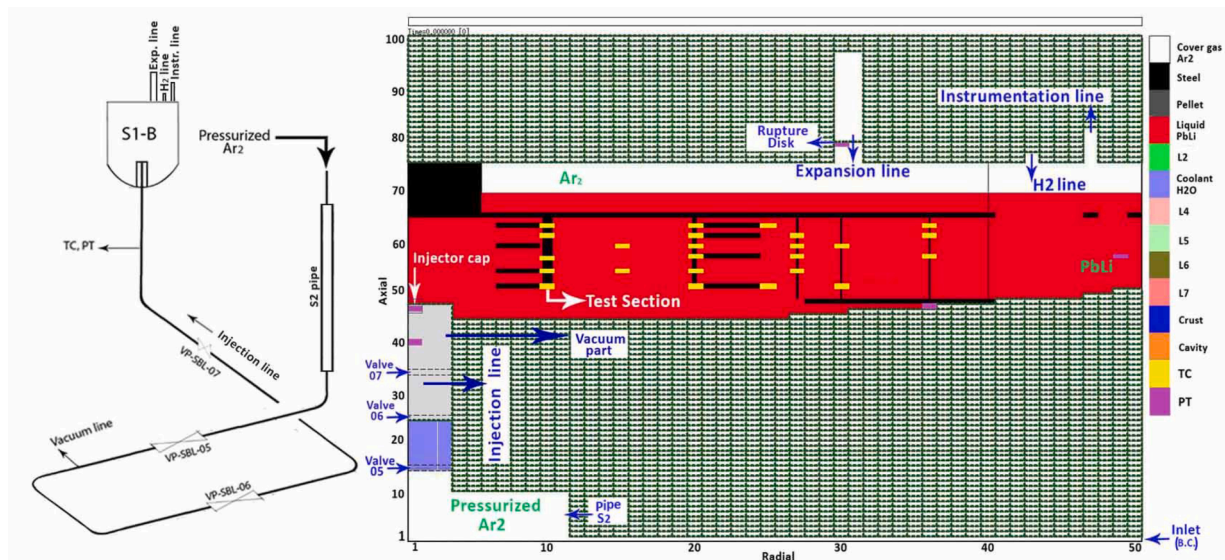
Phase 1. Pressurization of the water injection line [from valve opening to injector cap rupture (0–37 ms)]: Water begins to flow and pressurize the pipeline upstream as soon as the VP-SBL-06 valve is opened. The valve opening timing is set to the start of the transient ($t = 0$ s).

To mimic the entrance of Argon gas from the cylinder via the line, time-dependent pressure conditions are imposed (based on

Table 2

LIFUS5/Mod3 Test 5.2 Input Boundary conditions and reference values (nominal values, actual values and used in simulation by SIMMER-III).

#	LIFUS5/Mod3	Test E5.2			Date 13-05-21
	Parameter	ID	Design	Actual	SIMMER-III
SYSTEM S1B					
S1-1	P @ SoT (bar)	PC-S1B-01	1	0.95	0.95
S1-2	T_{PbLi} @ SoT (°C)	–	330	334.1	334.1
S1-10	Rupture disk open time(s)	PC-BYP-01	–	–	Not occurred
SYSTEM SBL					
S2-2	P @ SoT (bar)	PC-SBL-01	155	141.6	141.6
S2-3	T @ SoT (°C)	TC-SBL-04	295	255.2	255.2
S2-7	Mass of water injected (g)	MT-SBL-01	9-40	54	70 (at the top of ruptured cap)
INJECTION SYSTEM					
I-1	Injection valve	–	VP-SBL-06	VP-SBL-06	Virtual wall at top of cell (I=1-3, J=25)
I-2	Start of injection (s)	–	0	0	0
I-3	Injection time (from cap rupture) (s)	–	1.5	1.442	–
I-4	Injector cap rupture instant(s)	–	–	0.037	0.037
I-7	Injection valve fully closed instant(s)	–	1.5	1.476	1.476
I-8	Injector nozzle orifice (mm)	–	1	1	1
I-9	Injector penetration (mm)	–	20	20	20

**Fig. 5.** LIFUS5/Mod3 Reaction vessel (S1B,) injection line (SBL), and thermal-hydraulic nodalization SIMMER-III.

experimental data) at the top side of the injection line; see node (50,1) in Fig. 5. The cap rupture instance is selected from experimental data, roughly 36 ms following the SOT for the simulation. The cap rupture is simulated by the disappearance of a virtual wall at the top of the cell (1,47). The pressurization profile of the injection line during this phase can be seen in Fig. 6 (a).

Phase 2. Water-PbLi interaction [37–1476 ms], from cap rupture to fully closed valve VP-SBL-06 (EoI): This phase may be divided into 3 sub-phases:

- 2a. from cap rupture until the final point of the first pressure peak, injected water flashes [37–40.7 ms].
- 2b. from the termination of the initial pressure peaks until the pressure slope shift, pressurization is dominated by thermodynamic interaction [40.7–400 ms]. Fig. 7 shows the pressure profiles in S1B observed by different pressure transducers (time range 0–6 s selected to indicate the initial pressure before SOT, cap rupture instant, first and second pressure peak amplitude and instant).
- 2c. Chemical reaction dominates pressurization [400 ms to 1476 ms], from pressure slope shift to completely closed valve VP-SBL-06 (EoI).

The major events and critical parameters during phase 2 are described in points below:

- In the reference cells of reaction vessel S1B zone (50, 56), the pressure peak approaches the 2 bar (Fig. 7). After that, the pressure drops for a very short duration.
- The pressure of the injected water rises quickly once the orifice opens, then falls as the pressure wave disperses throughout the reaction vessel (pressure peak is absorbed quickly due to the large compressibility of cover gas Argon above the PbLi region).
- The injected water's predicted mass flow rate (Fig. 6(b)) spikes at the same time as the pressure peak, then drops due to increased pressurization in the reaction vessel. The complete pressure and mass flow rate trends (SIMMER-III calculated and experimental) are shown in Fig. 6(a) and (b). Both SIMMER-III predicted and experimental outcomes have good agreement throughout the transient and can be seen in Fig. 6.
- Despite this, water is constantly injected until the phase finishes (1.476 s), and the mass flow rate rises again and decreases thereafter due to the pressurization of S1B. The amount of hydrogen produced throughout phase 2 is indeed insignificant, but it grows throughout the transient, reaching equilibrium after phase 3.

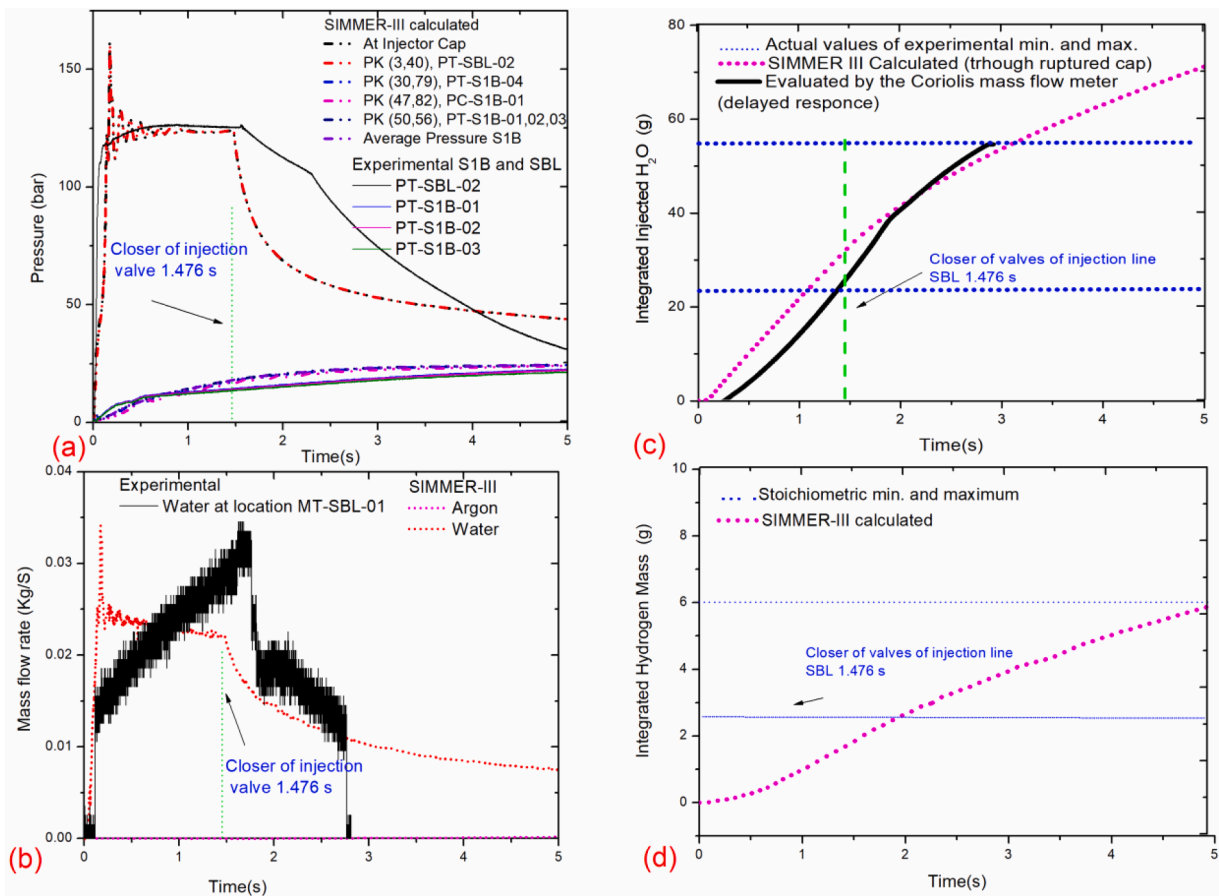


Fig. 6. (a) Pressure trends in the reaction vessel and Injection line, (b) Mass flow rate profile, (c) Integrated injected water profile during the transient and (d). Integrated hydrogen generated during the transient in the reaction vessel

- The code's calculations show that the lithium-water chemical reaction in phase 2a is still insignificant. During this phase 2a, the water-cooling effect significantly affects the temperature more than the heat generated by the chemical process (Fig. 8).
- Phase 2b and 2c: Starting at roughly 50 milliseconds, the pressure within S1B steadily increased to about 8 bar, owing to the water thermodynamic interaction with lead-lithium and evaporation of water. When valve VP-SBL-06 is closed, the pressure rises again, reaching 14bar.
- The pressurization caused by the exothermic chemical reaction between PbLi, and water and the subsequent hydrogen generation and temperature rise dominate this phase (see also the temperature trends in Fig. 5 inside the S1B reaction vessel). The total amount of water injected in S1B calculated by SIMMER-III is about 70 g, while the experimental value is about 54 g (Fig. 6(c)). Although nearly 6 g of hydrogen is produced (Fig. 6 (d)).

Phase 3. First pressure stabilization [1476 ms to ~2000 ms] from valve VP-SBL-06 fully closed (EoI) to first pressure stabilization. After valve VP-SBL-06 closure (it occurred at 1.476 s, see Fig. 6), the reaction vessel S1B was isolated from the SBL, but still, the injection line holdup water, which is at higher pressure, is connected to the reaction vessel S1B through the broken injection cap, which causes more water injection into the reaction vessel. From Fig. 6(c), we can see the residual amount of water injected from the injection line after VP-SBL-06 is fully closed, which causes further pressurization after the injection stops, but pressure increases due to this process are meager compared to the chemical reaction.

In the meantime, in the reaction vessel, the pressure increased from

14 to about 23 bars due to the chemical reaction of the PbLi with the amount of water still un-reacted. However, the effect was very bland. Furthermore, temperatures in the reaction vessel did not increase during this period.

Phase 4. Pressurization dominated by chemical reaction (2000–5000 ms) The pressure in the S1B reaction vessel continued to increase for two factors: first, it tended to equalize with the pressure within the injection line (this contribution, however, is restricted due to the injection line's small volume, particularly in comparison to the reaction vessel), and second, it was caused by the chemical reaction, the most significant contribution. Consequently, the temperatures in the reaction zone rose slowly again (see Fig. 8), and hydrogen release contributed to the pressure rise without a significant rate change. Due to the early cap rupture, pressure equalization between S1B and the injection line downstream (VP-SBL-06) occurs around $t = 6$ s. However, stabilization occurs at a gradual rate drop, and the plateau is only reached at EoT, which is not studied in the current manuscript due to convergence issues.

Fig. 9 provides a detailed picture of the rate of chemical reaction, water consumed in the chemical reaction of lead-lithium and water, and remaining water in reaction vessel during the transient. The water consumed in Fig. 9 is calculated by subtracting the amount of water present into the reaction vessel from the amount of water injected (liquid + vapor) at all time steps during the transient while considering the optimized reaction rate 10^{-3} into the code. The integrated injected water is calculated at the top of the orifice. While the water present in the reaction vessel is calculated by utilizing SIMBF input and bfc module of SIMMER-III code. From the water consumed profile in Fig. 9 we can easily depict the hydrogen generation profile.

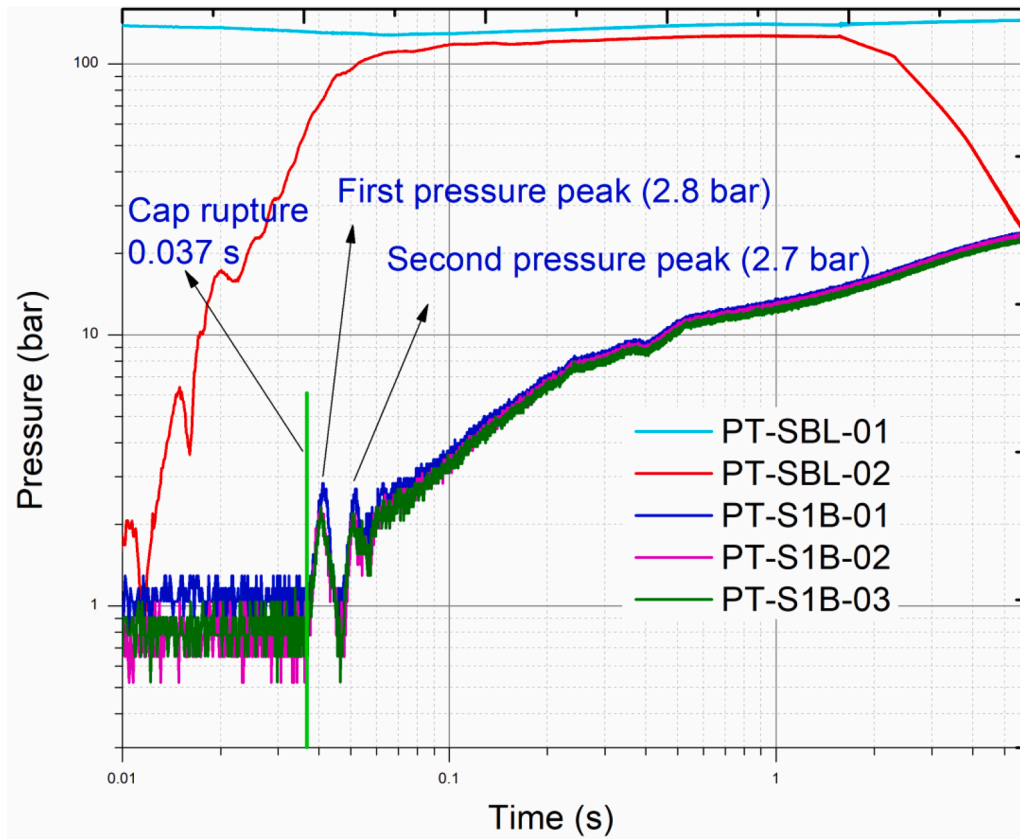


Fig. 7. Test E5.2, Pressure profile S1B observed by different pressure transducers.

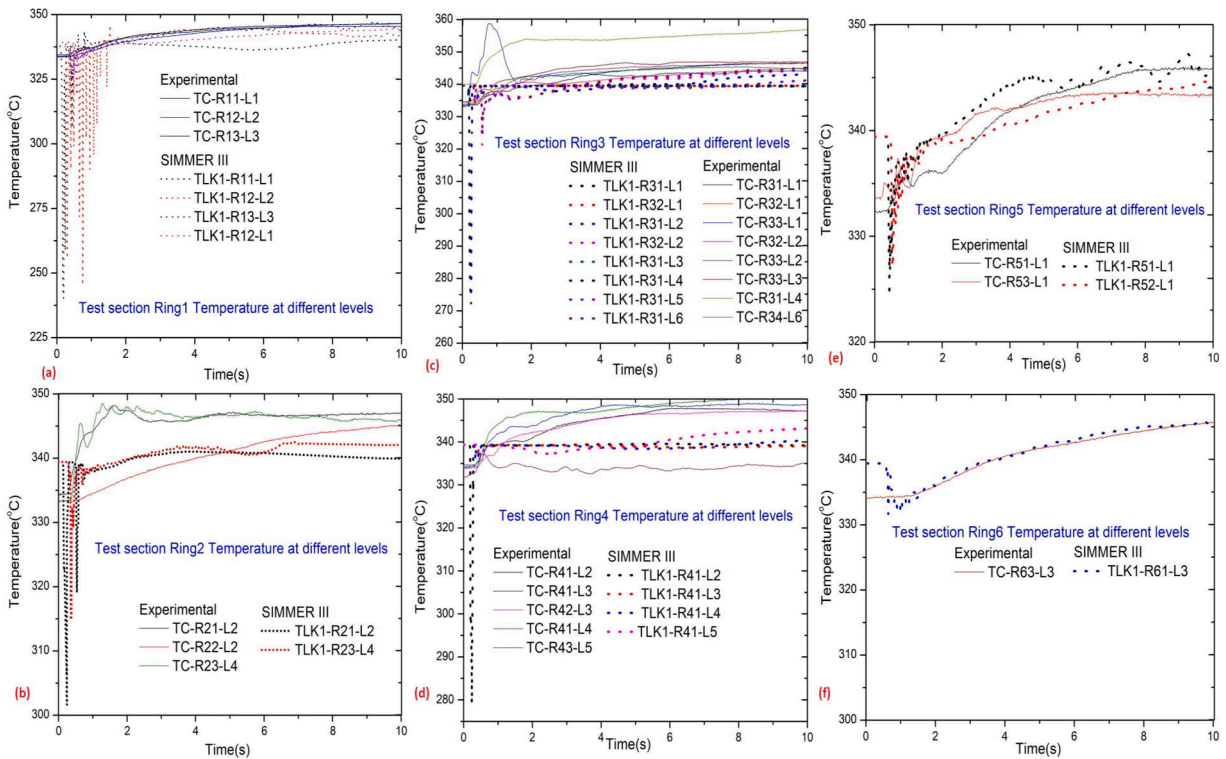


Fig. 8. Temperature trends in reaction vessel S1B at various locations (a) Ring 1, (b) Ring 2, (c) Ring 3, (d) Ring 4, (e) Ring 5 and (f) Ring 6.

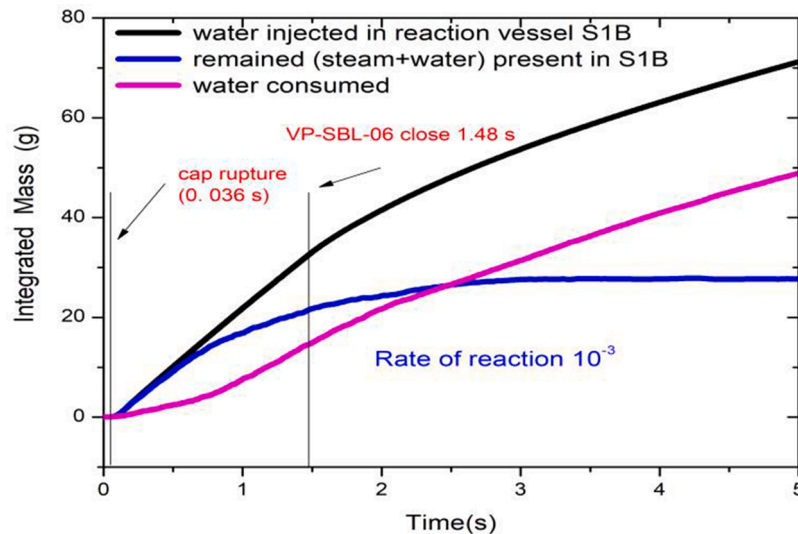


Fig. 9. Various governing parameters of chemical reaction in reaction vessel S1B.

5. Conclusions

The Test LIFUS5/Mod3 E5.2 was executed on May13th 2021 based on the planned Test matrix. The goal of Test E5.2 was met, and the data collected helped to expand existing databases for code validation. The thermo-hydraulic data analysis resulted in a full understanding of the processes that occurred during the Test, as well as the definition of starting and boundary conditions. Experimental Test permitted to obtain reliable data to be used for the validation of the modified version SIMMER codes for fusion application and of the coupled RELAP5/SIMMER approach [22].

The simulation of experiment E5.2 by system code SIMMER-III is successfully performed and compared with the experimental data by utilizing the initial boundary conditions used during the experiment execution. The best-optimized findings are reported in this publication after many runs of adjusting the sensitive and irregular parameters (like orifice discharge coefficient and coefficient of chemical reaction rate). Throughout the transient, there is excellent agreement between the simulation results and the experimental findings for the key parameters (pressure and temperature trends in the reaction vessel). It confirms the code's ability to forecast the behavior of thermodynamic and chemical interactions, particularly under the circumstances of this specific experimental Test E5.2

The results of post-test stand-alone simulation of Test E5.2 with SIMMER-III system code can be summarized as follows:

1. The Test demonstrated the phenomenon of the PbLi/water chemical interaction, in which the thermodynamic phenomena is the dominant process throughout the first few milliseconds after the cap rupture, followed by the secondary process, which involves a chemical reaction that produces hydrogen and a temperature rise. The pressure trends and temperature profiles in reaction vessel S1B and SBL calculated by the SIMMER-III code are quite comparable with the experimental trends (Figs. 6–8).
2. In Test E5.2, the cooling effect introduced by the flashing of water and its expansion is only present for a very short time, settles to a steady state, and then gradually increases over time, as seen in the simulation findings in Fig 8. The water jet's form, which is practically spread when injected into the melt, is responsible for this. Another factor might be that just in between 40 g to 54 g (uncertain due to delayed response of the Coriolis mass flow meter) of water was injected over a lengthy period (1.44 s).

3. The chemical reaction occurred between PbLi and water at the interface between the two fluids. The temperatures exhibit some notable peaks and hot patches during the initial phase, but in the later stage of the transient, these peaks disappear when the steam jet is nearly dispersed throughout the PbLi melt in the later phase (after 2 s; see Fig. 8). The heat released by the chemical reaction raised the temperature throughout the system.
4. According to temperature trends (Fig. 8), the level-4 ring-3 thermocouple (TC-R31-L4) measured the maximum temperature at EoT (369.53 °C), while the level-5 ring-3 thermocouple measured the lowest temperature at EoT (321.32°C) (TC-R33-L5) which is very well matched with the simulation results.
5. Integrated mass and temperature of injected water directly influence the chemical reaction, hydrogen production and the melt temperature.

Declaration of Competing Interest

The authors declare the following financial interests/personal relationships which may be considered as potential competing interests: None.

Data availability

The data that has been used is confidential.

Acknowledgments

This work has been carried out within the framework of the HORIZON2020, Call H2020-MSCA-IF-2020, funded by the European Research Executive Agency (REA) via the Marie Skłodowska-Curie Actions (Grant Agreement No 101030496). Although all the experimental facilities for the experimental campaign are made available by ENEA Brasimone Research Centre. Views and opinions expressed are, however, those of the author(s) only and do not necessarily reflect those of the European Union or the European Commission. Neither the European Union nor the European Commission can be held responsible for them.

References

- [1] A. Del Nevo, et al., Recent progress in developing a feasible and integrated conceptual design of the WCLL BB in EUROfusion project, Fusion Eng. Des. (2019), <https://doi.org/10.1016/j.fusengdes.2019.03.040>.

- [2] A. Del Nevo, et al., WCLL breeding blanket design and integration for DEMO 2015: status and perspectives Fusion, Eng. Des. 124 (2017) 682–686, <https://doi.org/10.1016/j.fusengdes.2017.03.020>.
- [3] E. Martelli, et al., Advancements in DEMO WCLL breeding blanket design and integration, Int. J. Energy Res. 42 (1) (2018) 27–52, <https://doi.org/10.1002/er.3750>.
- [4] M. Eboli, et al., Post-test analyses of LIFUS5 Test#3 experiment, Fusion Eng. Des. 124 (2017) 856–860, <https://doi.org/10.1016/j.fusengdes.2017.03.046>.
- [5] M. Eboli, et al., Experimental activities for in-box LOCA of WCLL BB in LIFUS5/Mod3 facility, in: Proceedings of the 30th symposium on Fusion Technology, September, 2018, <https://doi.org/10.1016/j.fusengdes.2019.01.113>.
- [6] M. Eboli, et al., Experimental and numerical results of LIFUS5/Mod3 series E test on in-box LOCA transient for WCLL-BB, Energies 14 (2021) 8527, <https://doi.org/10.3390/en14248527>.
- [7] S. Khani, et al., Post-test analysis of series D experiments in LIFUS5/Mod3 facility for SIMMER code validation of WCLL-BB In-box LOCA, Fusion Eng. Des. (2021).
- [8] S. Khani, M. Eboli, N. Forgiione, D. Martelli, A. Del Nevo, Validation of SIMMER-III code for in-box LOCA of WCLL BB: Pre-test numerical analysis of Test D1.1 in LIFUS5/Mod3 facility, Fusion Eng. Des. (2019), <https://doi.org/10.1016/j.fusengdes.2019.01.131>.
- [9] S.P. Saraswat, P. Munshi, A. Khanna, C. Allison, Thermal hydraulic and safety assessment of first wall helium cooling system of a generalized test blanket system in ITER using RELAP5 code, ASME J. Nucl. Rad. Sci. 3 (1) (2016), 014503, <https://doi.org/10.1115/1.4034680>.
- [10] S.P. Saraswat, P. Munshi, A. Khanna, C. Allison, Thermal hydraulic and safety assessment of LLCB test blanket system in ITER using modified RELAP/SCDAPSIM/MOD4.0 Code, ASME J. Nucl. Eng. Radiat. Sci. 4 (2) (2018) 021001–021010, <https://doi.org/10.1115/1.4038823>.
- [11] A. Pesetti, A. Del Nevo, N. Forgiione, Experimental investigation and SIMMER-III code modelling of LBE–water interaction in LIFUS5/Mod2 facility, Nucl. Eng. Des. 290 (2015) 119–126, <https://doi.org/10.1016/j.nucengdes.2014.11.016>.
- [12] A. Del Nevo, et al., Addressing the heavy liquid metal – Water interaction issue in LBE system, Prog. Nucl. Energy 89 (2016) 204–212, <https://doi.org/10.1016/j.pnucene.2015.05.006>.
- [13] M. Eboli, N. Forgiione, A. Del Nevo, Implementation of the chemical PbLi/water reaction in the SIMMER code, Fusion Eng. Des. 109–111 (2016) 468–473, <https://doi.org/10.1016/j.fusengdes.2016.02.080>.
- [14] AA.VV., SIMMER-III (Version 3.F) Input Manual, O-arai Engineering Center, Japan Nuclear Cycle Development Institute, 2012. May.
- [15] M. Eboli, A. Del Nevo, A. Pesetti, N. Forgiione, P. Sardain, Simulation study of pressure trends in the case of loss of coolant accident in water cooled lithium lead blanket module, Fusion Eng. Des. 98–99 (2015) 1763–1766, <https://doi.org/10.1016/j.fusengdes.2015.05.034>.
- [16] C. Blanchard, Modelling of the Lithium-lead/water interaction, improvement of the kinetics of the pressure evolution, 2022 CEA H0-200-5010-3090.
- [17] AA.VV., SIMMER-SW, Japan Nuclear Fuel Development Institute, JNC TJ9440 99-009, 1999.
- [18] I.E. Idelchik, Handbook of Hydraulic Resistance, 3rd ed., Jaico Publishing House, 2003.
- [19] S.P. Saraswat, P. Munshi, A. Khanna, C. Allison, Non-hyperbolicity of conservation equations Of RELAP5 two fluid model in nuclear reactor safety results – part i: investigation and eigenvalue analysis, ASME J. Nucl. Rad. Sci. 3 (1) (2020), <https://doi.org/10.1115/1.4047161>, 014503-014503-7.
- [20] S.P. Saraswat, P. Munshi, C. Allison, Characteristics and linear stability analysis of RELAP5 Twofluid model for two-component, two-phase flow, Ann. Nucl. Energy 151 (2020) 101–121, <https://doi.org/10.1016/j.anucene.2020.107948>.
- [21] S.P. Saraswat, P. Munshi, C. Allison, Linear stability analysis of RELAP5 two-fluid model in nuclear reactor safety results, Ann. Nucl. Energy 149 (2020) 101–117, <https://doi.org/10.1016/j.anucene.2020.107720>.
- [22] F. Galleni, S. Moghanaki, M. Eboli, A. Del Nevo, S. Paci, R. Ciolini, R. Lo Frano, N. Forgiione, RELAP5/SIMMER-III code coupling development for PbLi-water interaction, Fusion Eng. Des. 153 (2020), 111504, <https://doi.org/10.1016/j.fusengdes.2020.111504>. ISSN 0920-3796.